International Journal of Computer Science and Applications

Vol. 9, No. 3, pp. 108 – 127, 2012

A COMPUTER APPLICATION FOR 3D CRANIOFACIAL RECONSTRUCTION AND AUTOMATIC SKULL-PHOTO IDENTIFICATION

DAVID GARRIDO

CeDInt-UPM, Universidad Politécnica de Madrid, Edif. CeDInt-UPM Campus de Montegancedo, Madrid, 28223, Spain
dgarrido@cedint.upm.es
www.cedint.upm.es

LETICIA CARNERO

CeDInt-UPM, Universidad Politécnica de Madrid, Edif. CeDInt-UPM Campus de Montegancedo, Madrid, 28223, Spain
lcarnero@cedint.upm.es
www.cedint.upm.es

BELÉN RÍOS

CeDInt-UPM, Universidad Politécnica de Madrid, Edif. CeDInt-UPM Campus de Montegancedo, Madrid, 28223, Spain
brios@cedint.upm.es
www.cedint.upm.es

CARMEN LASTRES

CeDInt-UPM, Universidad Politécnica de Madrid, Edif. CeDInt-UPM Campus de Montegancedo, Madrid, 28223, Spain
clastres@cedint.upm.es
www.cedint.upm.es

Human identification from a skull is a critical process in legal and forensic medicine, especially when no other means are available. Traditional clay-based methods attempt to generate the human face, in order to identify the corresponding person. However, these reconstructions lack of objectivity, since they depend on the practitioner. On the other hand, superimposition of a skull with antemortem photographs is another popular method for suggesting individual identification; nevertheless, it is a costly process in terms of time if many photographs have to be analyzed. This paper presents two Human identification techniques. First one is an objective 3D craniofacial reconstruction method, without using any facial template. The only information required is the 3D image of the skull, age, gender and Body Mass Index of the individual. The second technique is an automated skull-photo superimposition method which calculates the matching degree of a large number of photos with a skull.

Keywords: Human identification; objective 3D craniofacial reconstruction; automatic skull-photo superimposition;

1. Introduction

The identification of human osseous remains can be carried out in many different ways. In this paper, a computer application that combines two procedures is proposed: the craniofacial reconstruction from the skull, and the comparison of the skull with a large set of photographs.

The goal of forensic craniofacial reconstruction is the identification of human and osseous remains, estimating the facial appearance of the individual associated to an unknown skull. It is a critical process in legal and forensic medicine, especially when no other means are available to identify the person [Wilkinson (2004)]. So far, this task has been performed by traditional 'plastic' methods, using clay. This process is carried out by an artist, who models the soft tissue knowing tissue depth in some landmark points on the skull. Depths elsewhere are interpolated between these points by intuition. In that process, replicas of real skulls are used, in order to avoid damaging them [Wilkinson (2004)]. This procedure has important disadvantages: on the one hand, it is an artistic method, which means the process is subjective. In fact, it is non-repeatable, since obtained results always differ between practitioners, and also between reconstructions. On the other hand, the technique is slow, and it usually takes one or two days, even for skilled practitioners. The method is also dirty and expensive, due to the materials required. In fact, a repetition of the process (the creation of a new reconstruction from the same skull using different individual parameters) means the use of new additional materials. Finally, the generated reconstructions are not easily transportable, which makes difficult their distribution or sharing.

All these disadvantages result in an increasing importance of the computer based facial reconstruction techniques [Greef and Willems (2005)]. Based on this fact, several works and proposals have been developed from the 90's until nowadays [Shahrom, *et al.* (1996), Liang, *et al.* (1996)]. They all suggest the different advantages of computerized 3D craniofacial reconstruction: it is a consistent process (the output results are the same when the same input data is used), and objective (it does not depend on any practitioner). Moreover, computerized methods can be executed in a short time, and they do not require extra material resources to repeat the reconstruction process from the same skull. All the previous facts make computer based methods better than traditional procedures.

Current computer based reconstruction techniques build the final reconstruction starting from a reference facial model. Most published computerized techniques ([Shahrom, *et al.* (1996), Tyrrel, *et al.* (1997) , Liang, *et al.* (1996)], e.g.) use a generic facial template, or a specific best look alike template, based on several subject properties (BMI, gender and age). This reference template is then fitted to the target skull knowing tissue thickness in some landmarks on that skull, and interpolating thickness in between these reference facial points, based on a generic smooth deformation. Finally, they add some extra information to improve the results, such as manual modeling features (nose, eyes, etc.) or a texture simulating the skin. The main problem of these procedures is they focus on human resemblance, instead of reliability: using a specific facial template, unwanted facial features of that template remain visible in the final reconstruction.

Besides, applying a generic deformation means a problem when the differences between the reference depth tissue values in landmarks and the reference face thickness are considerably large. On the other hand, the results are not skull specific, but just "smooth".

In attempt to solve the previous shortcomings, some techniques ([Subsol and Quatrehomme (2005)], for example) use specific deformations over the generic facial template. This deformation is obtained from a reference skull, which is deformed towards the target skull. Then, that deformation is extrapolated and applied to the facial template. Other computer based facial reconstruction proposals (for instance [Tu, *et al.* (2005), Vandermuelen, *et al.* (2006), Claes, *et al.* (2005)], instead of starting from a generic facial surface, they build a reference statistical model from a database of 3D scanned real faces. Thus, the problem of unrealistic and unreliable characteristics of the reconstructions is minimized.

All the previous methods and their results are limited, though, in the shape of the reference facial template they use to build the final craniofacial reconstruction: the output results will always contain specific features present in the reference template, which may distort the physical appearance of target person to identify. In addition, those techniques only use the information given by some points on the skull, instead of considering the complete skull surface; this disregards any individual particularity which should affect the final reconstruction morphology. Moreover, all these techniques require high complexity databases and procedures to perform the final reconstruction. In order to decrease complexity, and to avoid any unsuitable information which may be introduced by that reference facial surface, and also trying to consider as much information as may provide the skull geometry, we propose an alternative computer based craniofacial reconstruction technique, which is not based on a reference facial template. This reconstruction technique has been implemented in an application, which only starts from anthropological information, consisting in statistical soft tissue depth values in a set of points on the skull. Thus, complexity of the application database is considerably reduced. The only input data required by the application to generate the facial soft tissue mesh are the 3D image of the target skull, and a set of parameters of that skull: age, gender and BMI range. Facial features (eyes, nose, ears and mouth) are not included in the generated reconstruction, as they cannot be confidently deduced only from skull [Wilkinson (2004)].

Regarding the second procedure, the comparison of a skull with a large set of photograph, it is a popular human identification method for suggesting individual identification of unidentified human remains, also known as skull-photo superimposition. Superimposition is a technique that is often included among the methods of forensic facial reconstruction. The only shortcoming is that investigators must already have some kind of knowledge about the identity of the skeletal remains they are dealing with (as opposed to 2D and 3D reconstructions, when the identity of the skeletal remains is generally completely unknown). Forensic superimpositions are created by superimposing a photograph of an individual (supposed to belong to the unidentified skeletal remains) over an X-ray of the unidentified skull. If the skull and the photograph are of the same

individual, then the anatomical features of the face should align accurately [Lundy (1986)].

In the following section, a general description of the application is presented. Sections 3, 4, 5, 6 and 7 concentrate on examining the five main functional modules in the application: Landmark Insertion Module, Skin Mesh Generation Module, 2D Points Insertion Module, Homograph Module and Matching Module. Then, in Section 8, a comparison of different results is presented. Finally, Section 9 discusses the conclusions of the computer based facial reconstruction and skull-photo superimposition techniques here presented.

2. Application Description

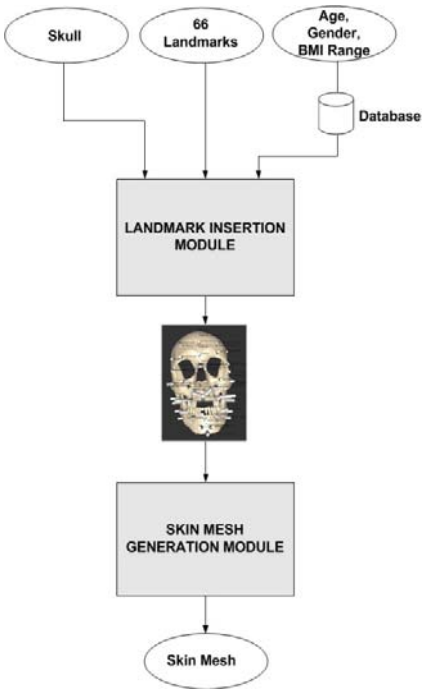

Fig. 1. 3D Face Reconstruction scheme.

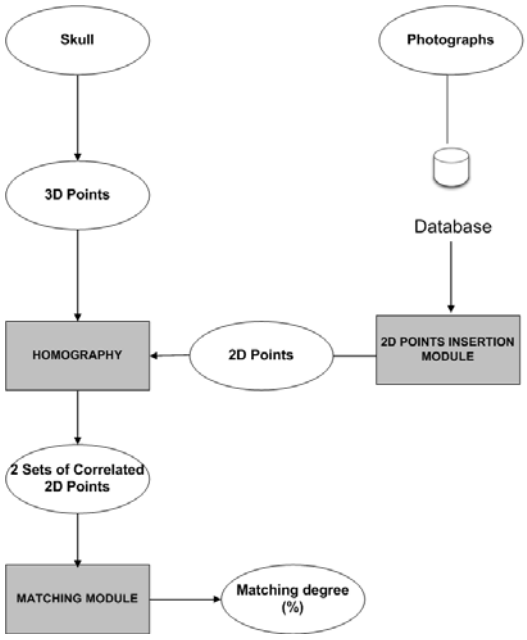

Fig. 2. Skull-Photo Superimposition scheme

2.1. *3D Face Reconstruction*

The 3D Reconstruction application presented in this paper can be represented by the scheme shown in Fig. 1.

The application input data is introduced by the final user (the forensic doctor). It comprises the following elements: firstly, a 3D image of the target skull. Secondly, 66 landmark points placed on the skull surface, where soft tissue depth is known (user will be able to decide whether introducing these positions manually or automatically by the

application). The last input data required by the application is a set of characteristic parameters of the target person: age, gender and BMI range. Age and gender can be deduced from skull morphology [Wilkinson (2004)], so they will always be known by the user. However, BMI range will be an unknown parameter, which will have to be estimated.

The Landmark Insertion Module is in charge of placing each landmark point in each position over the skull, and assigning the corresponding soft tissue depth value, according to age, gender and BMI parameters. This functional block will be further described in Section 3 of this paper.

Finally, the Soft Tissue Generation Module is the responsible for generating the skin mesh from the set of landmarks, where soft tissue depth is known. This block will be analyzed in Section 4. The application database consists of a set of tissue depth values in each reference point, varying according to age, gender and BMI attributes. This fact means that the database complexity is very small compared to those consisting of CT images, as in [Tu, *et al.* (2005), Vandermuelen, *et al.* (2006), Claes, *et al.* (2005)].

2.2. *Skull-Photo Superimposition*

The Skull-Photo superimposition application presented in this paper can be represented by the scheme shown in Fig. 2.

The application input data is introduced by the user (the forensic doctor). It comprises the following elements: firstly, a 3D image of the target skull. Secondly, 5 landmark points placed on the skull surface. The last input data required by the application is an undefined number of photos (one at least) which are located in a database server. The user has the possibility to select only a specific set of photos to be compared (when some a priori knowledge exists on the possible individuals to be identified) or even all the photographs stored in the database.

The 2D Points Insertion Module is in charge of placing automatically each 5 points in the correct position on the photograph. This functional module will be further described in section 5 of this paper.

The Homography Module is the responsible for taking both sets of points (skull points and photograph points) and performs a homography transformation which relates the coordinate system of skull points with coordinate system of photograph points. This module will be described in section 6 of this paper.

Finally, the Matching Module calculates the degree of correspondence between these new sets of points which are in the same coordinate system by applying different mathematical algorithms described in section 7.

3. Landmark Insertion Module

The Landmark Insertion Module (LIM) is in charge of placing 66 reference points on the skull surface, and assigning them a tissue depth value, based on a set of parameters of the person: age, gender and BMI range (previously introduced by the user in the system via

the graphic user interface). The reference points used for this purpose are two sets of points traditionally used in forensic medicine, as depicted on Fig. 3.

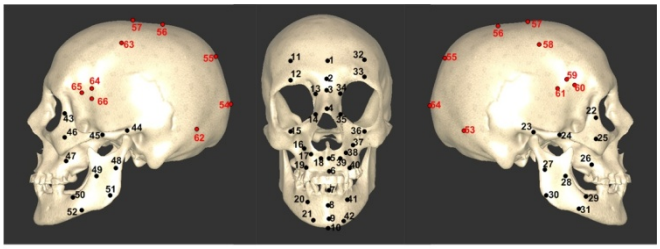

Fig. 3. Landmark definition used for craniofacial reconstruction in this work (left, front and right views). In black: set of 52 points to generate the facial reconstruction in facial zone [Greef, *et al.* (2006)]. In red: set of 14 points to generate the craniofacial reconstruction in neurocranium [Moore-Jansen, *et al.* (1994)].

The first set (black points on Fig. 3) results from an anthropological study, presented in [Greef, *et al.* (2006)]. They are compulsory points, since they make possible to generate soft tissue in frontal and lateral sides of a skull. However, that set of points would leave empty the top and the back of the skull. A second set of points has been considered to generate soft tissue around the whole skull (see red points on Fig. 3). That set of points has been selected in characteristic positions on the skull so that any user can recognize them unequivocally. Moreover, the soft tissue depth variations in that zone can be disregarded, and their magnitude can be approximated by tissue depth in point 1.

Based on the previous fact, the system will take 66 positions on a skull 3D image, and the age, gender and BMI range of that person (which will be introduced via the graphic user interface). Then, tissue thickness will be determined in all those reference points according to the parameters of the person. In the following subsections, these two processes (landmark insertion and tissue depth load) are analyzed.

3.1. *Landmark Insertion*

The landmark insertion process places the set of 66 reference points on the skull 3D image. Two different ways to accomplish this task have been implemented: manually and automatically.

In the manual procedure, user inserts all landmarks directly on the skull image. The list of 66 reference points is displayed in the graphic user interface, via a combo box element. The user only has to select one reference point and click on the skull image on its corresponding position. The procedure is independent of the order of selection.

In the automatic procedure, all the landmarks will be placed automatically on the image. In order to perform that task, the skull 3D image is projected on the front, right and left planes, and landmark positions are calculated into these projection planes, since those positions are quasi invariant in every skull. For this purpose, the skull needs to be oriented previously, in order to place it in front position respect to viewer camera. Once

all points have been placed on the projected images, an inverse transformation is applied over them to recover the whole 3D image, with all the landmarks placed on it. Likewise, user is allowed to modify any resultant position, if inaccurate.

3.2. *Tissue Depth Load*

Once all reference points have been placed on the skull 3D image, tissue thickness is assigned to each one, according to the age, gender and BMI range parameters previously introduced. Soft tissue depth values in reference points are known thanks to an anthropological study to characterize tissue depth information of Spanish population, performed by Legal Medicine School of Madrid, and based on a previous study of Belgian population [Greef, *et al.* (2006)]. This study is still in progress, and until this moment, it has been carried out with 160 people, men and woman, aged between 20 and 90 years old. Tissue thickness values are classified into several groups: according to gender, men and women; according to age, five groups can be found: between 20 and 29 years, between 30 and 39, between 40 and 49, between 50 and 59, and older than 60; and finally, according to BMI, population can be divided into 3 groups: people with BMI lower than 20, people with BMI between 20 and 25, and people whose BMI is higher than 25.

Considering this classification, 30 groups of population result. For each one, a tissue thickness mean value is available in the database for every landmark. Based on that fact, and depending on the gender, age and BMI range values of the corresponding person, the system will access to the corresponding entry in the database (population group and landmark), and will assign its depth value to each landmark.

4. Skin Mesh Generation Module

The Skin Mesh Generation Module (SMGM) represents the main functional module in the 3D Reconstruction application here presented. From output data generated in LIM, it manages to construct a full 3D mesh representing soft tissue (skin) belonging to the skull. The general aim of this module is to generate a set of intermediate points on the skull surface, whose depth values can be interpolated from thickness values in reference points. The whole set of points (landmarks and intermediate points) will integrate the final skin mesh. For this purpose, the module receives the set of 66 reference points (their positions and depths), and determines new tissue thickness values in each intermediate point, attending to its location (closeness to the rest of landmarks). For this reason, the presented craniofacial reconstruction technique considers all the information contained in the skull geometry, not only soft tissue thickness in the landmark points. Fig. 4 illustrates this procedure.

Therefore, the main functions participating in the whole process are the intermediate points generation and projection, the interpolation of intermediate depths and normals, and the soft tissue mesh generation. In the subsequent subsections, these four processes will be analyzed.

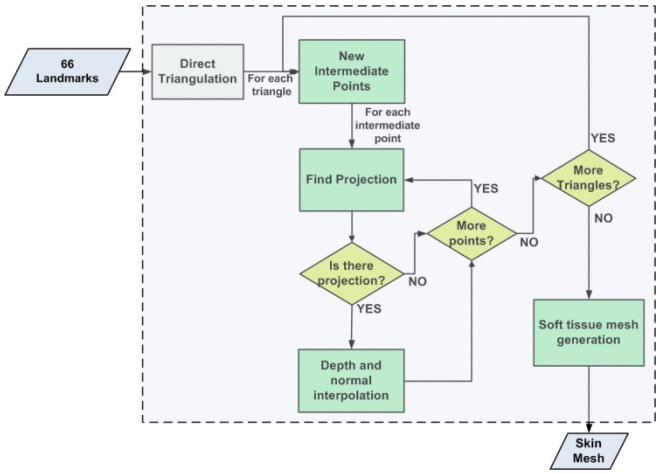

Fig. 4. SMGM block diagram.

4.1. *Intermediate Points Generation*

First step in skin mesh generation process is the creation of a set of new intermediate points, which will integrate the resulting final mesh. Those new intermediate points are created by using a new triangulation (transparent to the user). In a further process, those new generated points will be projected towards the skull geometry, so that new tissue depth can be obtained on them.

Therefore, the whole process of intermediate point generation comprises two main tasks: the construction of the reference triangle network, and the creation of the new intermediate points in those reference triangles. First task is carried out from the 66 landmarks positions. Then, a manual triangulation is performed, to optimize the amount of resulting triangles, and their shape and distribution. Fig. 5 illustrates the definition of the reference triangle network.

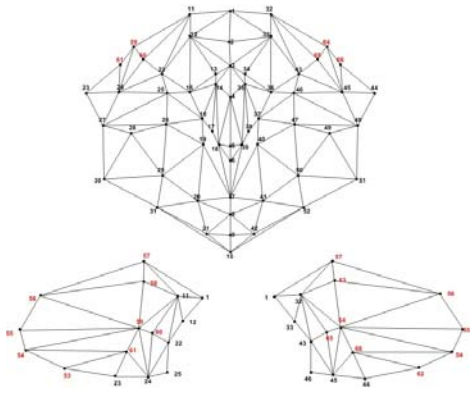

Fig. 5. Reference triangle network. The 52 facial points (black), and the 14 extra points (red) are indexed using the same numerical sequence as in Fig. 3.

Regarding the second task (creation of new intermediate points), for each resulting triangle, several intermediate positions are calculated, both inside the triangle and on its edges. Creation of intermediate points in each edge consists in dividing that edge in equally sized segments. Generation of intermediate points inside each triangle attends to a regular triangle subdivision [Vlachos, *et al.* (2001)]. This triangle subdivision is performed according to the *level of detail*, LOD, defined as the number of evaluation points on one edge minus two. The number *n* of intermediate points generated inside a triangle can be obtained from LOD, following equation 1. Fig. 6 illustrates this relation.

$$n = \sum_{i=1}^{LOD-2} i \tag{1}$$

4.2. *Intermediate Points Projection*

Once a set of numerous intermediate points has been generated, next step is to project all those points on the skull surface, in order to obtain a set of intermediate points where soft tissue depth can be added. Projection process is different depending on the location of the intermediate point to be projected. Based on this fact, two types of projections are performed: projection of points inside a reference triangle, and projection of points in a triangle edge.

Projection of intermediate points located inside a reference triangle is performed using the normal vector of that triangle. Projection of intermediate points located on an edge will be carried out using the vector defined by equation 2:

$$\vec{p} = \overrightarrow{n_1} + \overrightarrow{n_2} \tag{2}$$

Where n_1 and n_2 are the normal vector of the triangles sharing that edge. In both cases, projection will not be performed unless the condition $d < d_{max}$ is satisfied, being d the distance between the original intermediate point and the point projected on the skull mesh, and d_{max} is a threshold value. This condition prevents an intermediate point from being projected too far from its 3 nearest landmarks, which constitute the reference triangle. This may happen in several regions, for example, inside eye sockets. It is a fundamental condition, since tissue depth associated to the new intermediate points on the skull mesh will be obtained0 from tissue depth values on those 3 nearest landmarks (as it will be described in section C). Therefore, it is very important to ensure all the projected points have the same landmark neighbors as their corresponding original intermediate point.

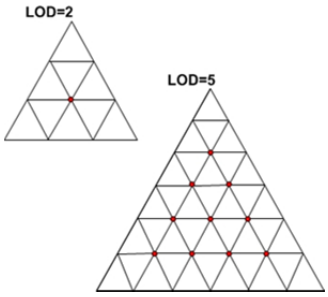

Fig. 6. Examples of inner triangle subdivision, with LOD=2 and LOD=5. Intermediate points are highlighted.

4.3. *Intermediate Depth and Normal Interpolation*

In the previous step, a set of intermediate points on the skull surface were calculated. Next task is to calculate their tissue depth values, in order to obtain the final set of points which will integrate the skin mesh. In all cases, an intermediate skin position can be obtained as:

$$\vec{p}' = \overrightarrow{p_i} + \overrightarrow{n_i} \cdot l \tag{3}$$

Where p_i is the position vector of the projected intermediate point, n_i is the normal vector in that point, and l_i the thickness associated to it. The way to compute l_i and n_i will differ, depending on the location of the original intermediate points in the reference triangles.

For skull intermediate points coming from projection of points located inside a reference triangle (p_i'), n_i and l_i are interpolated from l_1, l_2, l_3, and n_1, n_2, n_3, the depth and normal values associated to the three landmarks integrating the reference triangle (influence landmarks). The subsequent equations are used:

$$l_i = u \cdot l_1 + v \cdot l_2 + w \cdot l_3 \tag{4}$$

$$\overrightarrow{n_i} = u \cdot \overrightarrow{n_1} + v \cdot \overrightarrow{n_2} + w \cdot \overrightarrow{n_3} \tag{5}$$

$$u = \frac{area(\overrightarrow{p_i}', \overrightarrow{p_2}, \overrightarrow{p_3})}{area(\overrightarrow{p_1}, \overrightarrow{p_2}, \overrightarrow{p_3})} \tag{6}$$

$$v = \frac{area(\overrightarrow{p_1}, \overrightarrow{p_i}', \overrightarrow{p_3})}{area(\overrightarrow{p_1}, \overrightarrow{p_2}, \overrightarrow{p_3})} \tag{7}$$

$$w = \frac{area(\overrightarrow{p_1}, \overrightarrow{p_2}, \overrightarrow{p_i}')}{area(\overrightarrow{p_1}, \overrightarrow{p_2}, \overrightarrow{p_3})} \tag{8}$$

For skull intermediate points coming from projection of points located in a triangle edge (p_i'), n_i and l_i are interpolated from l_1, l_2, and n_1, n_2, those depth and normal values

associated to the two landmarks integrating that edge (influence landmarks). The following equations are used:

$$l_i = u \cdot l_1 + v \cdot l_2 \tag{9}$$

$$\overrightarrow{n_i} = u \cdot \overrightarrow{n_1} + v \cdot \overrightarrow{n_2} \tag{10}$$

$$u = \frac{distance(\overrightarrow{p_i'}, \overrightarrow{p_2})}{distance(\overrightarrow{p_1}, \overrightarrow{p_2})} \tag{11}$$

$$v = \frac{distance(\overrightarrow{p_1}, \overrightarrow{p_i'})}{distance(\overrightarrow{p_1}, \overrightarrow{p_2})} \tag{12}$$

4.4. *Mesh Generation*

Once the set of intermediate tissue points has been generated (from the original 66 landmarks), the next step is to build a 3D mesh from both sets of points. Considering that the final number of points is greater than 11000, an automatic triangulation algorithm is required. For this purpose, a Delaunay triangulation has been implemented. In Fig. 7, a skull and its point sets (landmarks and intermediate points) are shown. Fig. 8 and Fig. 9 shows some examples of reconstructions obtained from different skulls, by means of the proposed application.

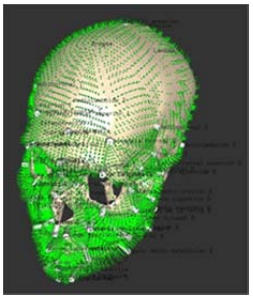

Fig. 7. Set of landmarks (white cylinders) and skin intermediate points generated (green spheres) for a generic skull.

Fig. 9. Examples of reconstructions using different skulls. (Left): 53-year-old man with BMI>25. (Right): 34-year-old man with BMI>25.

Fig. 8. Examples of reconstructions using the skull of a 27-year-old man. (Left): BMI<20. (Center): 20<BMI<25. (Right): BMI>25.

In the previous images, the achievements and limitations of this craniofacial reconstruction method can be detected. Regarding the achievements, zones where skull geometry shows soft variations are well reconstructed; this is the case of the forehead, the chin, the upper part and lateral faces of the nose. However, limitations can be found in zones where skull varies, for example, in zigomatic arch zones and near eyes and mouth, especially. In those zones, a greater number of landmarks would be needed, in order to obtain an appropriate soft tissue depth interpolation.

5. 2D Points Insertion Module

The 2D Points Insertion Module places the set of 5 reference points on the photograph in two different ways: manually and automatically.

In the manual procedure, user inserts all points directly on the photo image. The list of 5 reference points is displayed in the graphic user interface. The user only has to select one reference point and click on the photo on its corresponding position. The procedure is independent of the order of placement.

In the automatic procedure, all the points will be placed automatically on the image. This module has been implemented using an OpenCV library (Open Source Computer Vision) [OpenCV].

First step to make an automatic insertion of points is detecting the face in the photograph. Face detection [OpenCV FaceDetection] function is provided by OpenCV. It uses a type of object detector called Haar Cascade classifier [Viola and Jones (2001), OpenCV Cascade Clasification]. Given an image, the face detector examines each image location and classifies it as "face" or "not face". This algorithm has three major components: the representation of the image, the construction of the classifier and the sequential combination of increasingly complex classifiers (Cascade). This method does not work directly with image intensities, but it uses a series of features based on the basic functions of Haar [Haar (1910)], although more complex than this. To make the feature extraction computation faster at many scales, the integral representation of images is introduced, which can be processed using a few operations per pixel. The classifier is constructed by selecting a small number of important features using AdaBoost [Freund and Schapire (1995)]. This process trains the classifier with hundreds of views of the same object (faces in this case), both positive and negative examples of the same size.

Once the face area is detected in the photograph, eyes and nose area are calculated using a classifier trained for these specific objects. A rectangle area is used to represent the area where objects (face, eyes and nose) have been detected, as shown in Fig. 9.

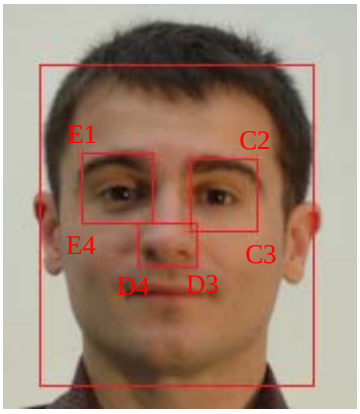

Fig. 9. Face, Eyes and Nose areas detected on photo.

Next step is to estimate the position of the set of 5 reference points These 5 points and their position in the photograph (see Fig. 10) have been provided by Legal Medicine School of Universidad Complutense of Madrid based on Bertillon's method [Bertillon (1889)].

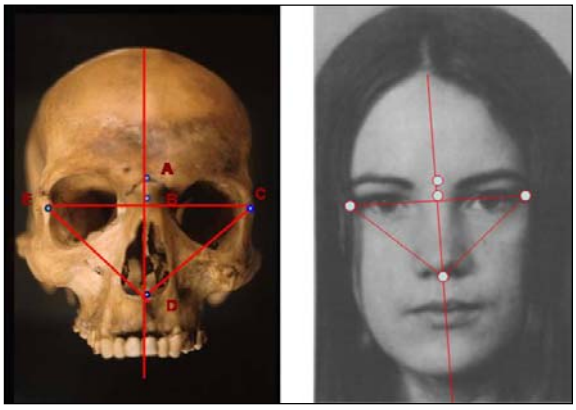

Fig. 10. Points Representation and their correlation.

The location of the areas where the eyes and nose are located is used to estimate the position of the five points. For example, point E (right eye) is calculated by taking the midpoint between E1 and E4 (see Fig. 9). Point C (left eye) is the midpoint between C2 and C3 (see Fig. 9). Point D is estimated by taking the middle distance between D3 and D4 (see Fig. 9). Point A is calculated by taking the middle point of the line formed by E1 and C2 (see Fig. 9). B is the intersection point between line formed by A-D and line formed by E-C points which have been calculated previously. A final estimation of these points is shown in Fig. 11.

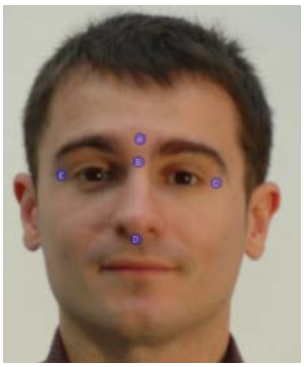

Fig. 11. Example of photo with final points calculated.

It is necessary to note that images used in Fig. 9 and Fig. 11 belong to a public data base of photographs [Tarrés and Rama]. Many other photos from this public data base have been used in tests and validation processes of the application.

6. Homograph Module

After estimating the position of the points on the skull and on the photograph, it is necessary to calculate the correlation between them.. The face in the photograph may not be in a perfect front position, it could be inclined or rotated and the insertion of points has to be done taking into account this two factors. The correlation between the two set of points is performed using a homography (see a graphic example of homography on figure 12).

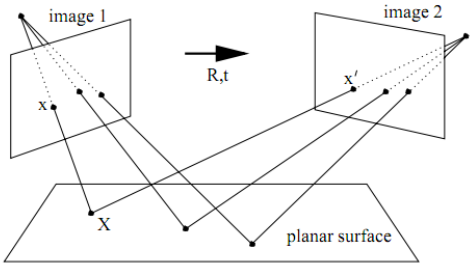

Fig 12: Example of homography between 2 sets of points.

The Homograph Module calculates the homograph transformation between the set of points from skull and the set of points from the photograph. Homography [Hartley and Zisseman (2000), Hartley and Zisseman (2003)] is a special projective transformation which relates the coordinate system x =[x1, x2] with u =[u1, u2] by:

$$x_1 = \frac{a_1u_1 + a_{12}u_2 + a_{13}}{a_{31}u_1 + a_{32}u_2 + a_{33}} \quad (13) \quad \text{and} \quad x_2 = \frac{a_{21}u_1 + a_{22}u_2 + a_{23}}{a_{31}u_1 + a_{32}u_2 + a_{33}} \quad (14)$$

OpenCV libraries have been used to implement the homography. The cvFindHomography function [OpenCV Homography], finds the perspective transformation between two planes taking two sets of points as input parameters. The third input parameter considered by this function is the method used to compute homography matrix. In this case, the RANSAC (Random Sample Consensus) algorithm is used [Fischler and Bolles (1981), Konstantinos (2010)]. RANSAC is a robust estimator for robust fitting of models in the presence of many data outliers. Unlike others algorithms that use as much of the data as possible, RANSAC uses the smallest data set possible to obtain an initial solution.

7. Matching Module

The Matching Module calculates the degree of correspondence between skull and photograph points after they have been correlated by the Homograph Module.
This degree of matching is calculated as follows:

Each point is considered as a 2D vector with (x, y) coordinates. Photograph points are named as pA, pB, pC, pD and pE. Skull points are named as sA, sB, sC, sD and sE. Two auxiliary points are calculated, pC_{aux} and sC_{aux}. These auxiliary points are the centroids of each set of points and they are calculated as follows (only equations for photograph points are shown):

$$pC_{aux} = \frac{pA+pB+pC+pD+pE}{5} \tag{15}$$

Next step is to calculate the distance between this centroid and each point:

$$D(pA, pC_{aux}) = \sqrt{(pA.x - pC_{aux}.x)^2 + (pA.y - pC_{aux}.y)^2} \tag{16}$$

The same equation has to be applied to the rest of points, pB, pC, pD and pE. In addition, the angle formed by each point and centroid is estimated:

$$\text{If } \left(-1 \leq \frac{pA*pC_{aux}}{\sqrt{pA.x^2+pA.y^2}*\sqrt{pC_{aux}.x^2+pC_{aux}.y^2}} < 1\right) \quad \text{then} \tag{17}$$

$$Ang(pA, , pC_{aux}) = \text{acos}\left(\frac{pA*pCaux}{\sqrt{pA.x^2+pA.y^2}*\sqrt{pCaux.x^2+pCaux.y^2}}\right) \tag{18}$$

The same equation is applied to pB, pC, pD and pE. Moreover, equations (15), (16), (17) and (18) presented above, are applied to points sA, sB, sC, sD and sE.

After that, the distance error between photo points and skull points is calculated as follows:

$$D_{ACerror} = \text{abs}\left(\frac{D(sA,sC_{aux}) - D(pA,pC_{aux})}{D(sA,sC_{aux})}\right) \tag{19}$$

This equation is applied to the rest of distances calculated previously ($D_{BCerror}$, $D_{CCerror}$, $D_{CDerror}$ and $D_{ECerror}$). Once these distances have been calculated, the average has to be computed:

$$\text{AvgDistError} = \frac{D_{ACerror} + D_{BCerror} + D_{CCerror} + D_{DCerror} + D_{ECerror}}{5} \quad (20)$$

Next step is to estimate the angle error:

$$\text{Ang}_{\text{ACerror}} = \text{abs}\left(\frac{Ang(sA,sC_{aux}) - Ang(pA,pC_{aux})}{2\pi}\right) \quad (21)$$

Once equation (21) is applied to all the points ($\text{Ang}_{\text{BCerror}}$, $\text{Ang}_{\text{CCerror}}$, $\text{Ang}_{\text{DCerror}}$ and $\text{Ang}_{\text{ECerror}}$), the average is calculated:

$$\text{AvgAngError} = \frac{Ang_{ACerror} + Ang_{BCerror} + Ang_{CCerror} + Ang_{DCerror} + Ang_{ECerror}}{5} \quad (22)$$

Moreover, the standard deviation of distance error (StandardDeviationErrorDistance) and standard deviation of angle error (StandardDeviationErrorAngle) are computed.

Then, the total standard deviation is calculated:

$$\text{TotalDeviation} = \frac{StandardDeviationErrorDistance + StandardDeviationErrorAngle}{2} \quad (23)$$

Finally, the percentage of matching between skull and photograph is estimated as follows:

$$\text{Matching (\%)} = \frac{1}{1 + TotalDeviation} * 100 \quad (24)$$

8. Comparison of Results

In this section, different results are presented, in order to prove that the craniofacial reconstruction method here described verifies these four statements: firstly, craniofacial reconstructions are different for different skulls. Secondly, they are different for a certain skull, using different BMI ranges. Thirdly, craniofacial reconstructions depend on the skull geometry, existing correspondence between skull morphology and skin mesh. And finally, the procedure is not subjective, since craniofacial reconstructions only depend on tissue thickness values in the 66 landmarks and skull geometry.

To perform the test, 145 3D-scanned skulls (69 women and 76 men) have been used: 4 samples aged between 20 and 29, 14 samples between 30 and 39, 9 samples between 40 and 49, 18 samples between 50 and 59, and 100 samples older than 60 years old.

Using these skulls, several reconstructions have been performed varying BMI range values in each skull. In order to contrast objectively all existing changes, two representative measures have been taken in each skull and its corresponding reconstruction: distance between landmarks 1 and 10 (facial length) and between

landmarks 23 and 44 (bizigomatic breadth). Table I shows the measures taken from 7 different sample skulls. Measures corresponding to BMI<20 are not presented due to the fact that there are not tissue depth values available in some population groups, since the anthropological database is still being completed.

Table 1. List of measures (in cm.) taken in 7 skulls and reconstructions.

Individual	**Distance 1-10 (facial length)**			**Distance 23-44 (bizigomatic breadth)**		
	Skull	**20<BMI<25**	**BMI>25**	**Skull**	**20<BMI<25**	**BMI>25**
25-year-old man	15.19	15.85	15.9	10.99	13.65	14.06
34-year-old man	16.18	17.17	17.26	11.64	13.24	13.85
39-year-old man	15.29	16.27	16.39	12.21	13.85	14.67
45-year-old woman	14.09	15.06	15.15	11.22	13.21	13.57
53-year-old man	15.42	16.62	16.9	12.2	14.23	14.59
73-year-old woman	14.18	15.37	16.45	11.9	13.65	13.87
75-year-old woman	14.51	16.62	16.7	11.15	12.96	13.24

According to those results, differences between reconstructions belonging to the same skull using different BMI values have been proved, and also differences between reconstructions from different skulls. Based on this fact, the objectivity of the present craniofacial reconstruction method can be ensured.

In order to improve the validation process of the proposed method and test its accuracy, some further tests are being performed to study the variations of the surface in the reconstruction meshes, in comparison with the variations corresponding to real skin meshes (extracted from TAC images). This process is still in progress, since there are not enough TAC images available to construct a reliable sample of real soft tissue.

Regarding the validation of the skull-photo superimposition process, it has been tested with a reduced number of skulls which their corresponding photographs are known. In these cases, the degree of correspondence with the correct photos is higher than the degree of correspondence with other photos. However, the validation process is still at a preliminary stage and more tests need to be done to confirm the success ration in the comparison process.

9. Conclusion

In this paper, two human identification methods have been presented. A graphic application has been developed implementing those techniques.

First technique enables to generate objectively the soft tissue of any individual, starting only from the skull and a set of 66 reference points where tissue depth is known.

The method consists in generating a great number of intermediate points, where tissue depth is interpolated from tissue thickness in landmark points. This process only comprises projections, normal calculations, arithmetic operations, and finally, a

triangulation to build the final reconstruction. Moreover, the complexity of the application database is low, as it only consists of a set of soft tissue thickness values in the reference points. These two facts contribute to the low computational cost of the application.

The presented craniofacial reconstruction technique was developed to ensure the objectivity of the process, since it only considers skull geometry and individual parameters (age, gender and BMI range). On the other hand, it extracts all the local information contained in the target skull, since its entire surface is sampled. This means an important advantage in regions with smooth variations (forehead and chin, for example), where every irregularity will affect the final reconstruction; otherwise, they would be disregarded in case of only considering the set of reference landmarks. However, in places where skull geometry is variant, this tendency to replicate the skull variations is not suitable and it must be improved. In those places, more landmarks would be necessary.

Tests with 145 skulls have been performed, in order to compare the corresponding generated reconstructions. Future work focuses on improving the validation process, comparing reconstructions with real skin meshes extracted from TAC images.

The second technique enables to compare a large number of photographs with a skull, giving as a result the matching degree of each one with the selected skull through the graphic application. The method takes the 3D target skull, a set of 5 reference 3D points from skull, all photographs located in a data base and a set of 5 reference 2D points from each photograph. Both set of points are automatically positioned on skull and photo and user intervention is not required for this step. Once the set of points has been positioned, two basic steps are performed to calculate the correspondence degree between the skull and the photo: first one consists on passing the two sets of points (3D and 2D sets) to a common base through an homography. Once all points are in the same space, a comparison method based on mathematical rules is applied to determinate the matching error between them (a low error means a greater correspondence).

This method has been developed to try to speed up and automate the traditional method used by forensic doctors making possible the comparison of a large number of photos with a skull with little user intervention.

Nowadays, this technique is in validation process. The main problem found is the lack of a database of real skulls with their corresponding photos. Until now, the tests have been performed with a set of 5 skulls with their corresponding photos, a huge number of skulls without photo and a large number of photos (alive individuals). On this basis, different tests have been made, obtaining some first results: if a skull, which has its own photo, is compared with all photos from the database, then the highest matching degree is obtained with its corresponding photo. The matching degrees calculated with the other photos are smaller, although some of them are not significantly smaller than the result obtained with the right photo. Other tests have been made using skulls which have no photo, where the matching degrees with random photos should be small. However, some of the results show matching degrees close to 80%. This means that the software module

returns false positives in some cases. This risk could be mitigated using more reference points (3D and 2D), thus obtaining a more accurate matching calculation.

Future work focuses on improving the validation process, using TAC's images from alive individuals, extracting the skulls' surfaces and comparing them with the photos from those individuals.

Acknowledgment

Authors would like to thank the Legal Medicine School of Universidad Complutense of Madrid, for having contributed with their knowledge on forensic anthropology.

References

Bertillon, A. (1889): Alphonse Bertillon's Instructions for Taking Descriptions for the Identification of Criminals and Others, by Means of Anthropometric Indications

Claes, P.; Vandermuelen, D.; Greef, S. D.; Willems, G.; Suetens, P. (2005): Statistically Deformable Face Models for Cranio-Facial Reconstruction, in Proceedings of the 4th International Symposium on Image and Signal Processing and Analysis, ISPA2005, S. Lonc˘aric´, H. Babic´, and M. Bellanger, Eds. Croatia, pp. 347– 352.

Fischler M.A.; Bolles R. C. (1981): Random Sample Consensus: A Paradigm for Model Fitting with Applications to Image Analysis and Automated Cartography. Comm. of the ACM, Vol 24, pp 381-395.

Freund, Y.; Schapire, R.E. (1995): A decision-theoretic generalization of on-line learning and an application to boosting. In Computational Learning Theory: Eurocolt '95, pages 23–37. Springer-Verlag.

Greef, S. D.; Willems G. (2005): Three-dimensional Cranio-Facial Reconstruction in Forensic Identification: Latest Progress and New Tendencies in the 21st Century, Forensic Science International, vol. 50, pp. 12-17.

Greef, S. D.; Claes, P.; Vandermuelen D.; Mollemans, W.; Suetens, P.; Willems, G. (2006): Large-scale in-vivo Caucasian facial soft tissue thickness database for craniofacial reconstruction, Forensic Science International, vol. 154, pp. S126-S146.

Haar, A. Z. (1910): "Theorie der orthogonalen Funktionensysteme", Mathematische Annalen, 69, pp 331–371.

Hartley R.; Zisseman, A. (2000): Multiple view geometry in computer vision, Cambridge University Press, Cambridge, UK

Hartley R.; Zisseman, A. (2003): Multiple view geometry in computer vision, Cambridge University, Cambridge, 2nd edition.

Konstantinos G. (2010): Overview of the RANSAC Algorithm, kosta@cs.yorku.ca Version 1.2 May 13.

Liang, R.; Lin, Y.; Jiang, L.; Bao, J.; Huang, X. (2009): Craniofacial Model Reconstruction From Skull Data Based on Feature Points, in Computer-Aided Design and Computer Graphics, CAD/Graphics '09. 11th IEEE International Conference Huangshan, pp. 602-605.

Lundy, K. J. (1986): Physical Anthropology in Forensic Medicine, Anthropology Today, Vol. 2, No. 5, pp. 14-17

Moore-Jansen, P. M.; Ousley, S. D.; Jantz, R. L. (1994): *Data Collection Procedures for Forensic Skeletal Material*, Forensic Antrhopology Center, Department of Anthorpology, University of Tennessee, Knoxville.

OpenCV, http://opencv.willowgarage.com/wiki/

OpenCV, Face Detection: http://opencv.willowgarage.com/wiki/FaceDetection

OpenCV, Cascade Clasification:
http://opencv.itseez.com/modules/objdetect/doc/cascade_classification.html

OpenCV, Homography:
http://opencv.willowgarage.com/documentation/cpp/calib3d_camera_calibration_and_3d_reconstruction.html?#findHomography

Shahrom, A. W.; Vanezis, P.; Chapman, R. C.; Gonzales, A.; Blekinsop, C.; Rossi, M. L. (1996): Techniques in facial identification: computer-aided facial reconstruction using a laser scanner and video superimposition, International Journal of Legal Medicine, vol. 108, pp. 194-200.

Subsol, G.; Quatrehomme, G. (2005): Automatic 3D facial reconstruction by feature-based registration of a reference head, in Computer-graphic Facial Reconstruction, J. G. Clement and M. K. Marks, Eds.: Elsevier Academic Press, pp. 145-162.

Tarrés, F.; Rama A.: GTAV Face Database,
http://gpstsc.upc.es/GTAV/ResearchAreas/UPCFaceDatabase/GTAVFaceDatabase.htm

Tu, P.; Hartley, R. I.; Lorensen, W. E.; Allyassin, M.; Gupta, R.; Heier, L. (2005): Face Reconstructions using Flesh Deformation Modes, in Computer Graphic Facial Reconstruction, J. G. Clement and M. K. Marks, Eds.: Elsevier Academic Press, pp. 145-162.

Tyrrel, A. J.; Evision, M. P.; Chamberlain, A. T.; Green, M. A. (1997): Forensic three-dimensional facial reconstruction: historical review and contemporary developments, Journal of Forensic Sciences, vol. 42, pp. 653-661

Vandermeulen, D.; Claes, P.; Loeckx, D.; Greef, S. D.; Willems, G.; Suetens, P. (2006): Computerized craniofacial reconstruction using CT-derived implicit surface representations, Forensic Science International, vol. 159, pp. 164-174.

Viola, P.; Jones, M. (2001): Rapid Object Detection using a Boosted Cascade of Simple Features, Computer Vision and Pattern Recognition.

Vlachos, A.; Peters, J.; Boyd, C.; Mitchel, J. (2001): Curved PN Triangles, symposiuim on Interactive 3D Graphics, New York, pp. 159-166.

Wilkinson, C. (2004): Forensic Facial Reconstruction, Cambridge University Press, New York.